Altered Voltage Dependence of Fractional Ca^{2+} Current in *N*-Methyl-D-Aspartate Channel Pore Mutants with a Decreased Ca^{2+} Permeability

Ralf Schneggenburger
Ecole Normale Supérieure, Laboratoire de Neurobiologie, 75005 Paris, France

ABSTRACT The Ca^{2+} permeability properties of an *N*-methyl-D-aspartate (NMDA) channel pore mutant (NR1E603K-NR2A) were studied using whole-cell patch-clamp recordings in human embryonic kidney cells. Measurements of reversal potential shifts indicated that the relative permeability of Ca^{2+} over monovalent ions, P_{Ca}/P_M, was 1.6, a value reduced by a factor of ~2 with respect to the wild-type channel. The ratio of Ca^{2+} current over total current (fractional Ca^{2+} current), however, was 19.7 ± 1% at −50 mV and 2 mM external Ca^{2+} concentration, a value similar to that of the wild-type channel, but 2.3-fold larger than that predicted by simple permeation models for the corresponding P_{Ca}/P_M value. The deviation from predicted values gradually disappeared with membrane depolarization. Similar results were obtained for two cysteine mutations at asparagine residues of the NR1 and NR2A subunits. When interpreted in terms of a two-barrier one-site model for ion permeation, the results indicate that changes in the relative Ca^{2+} permeability occur close to an internal energy barrier limiting ion permeation.

INTRODUCTION

The glutamate-activated channels of the *N*-methyl-D-aspartate (NMDA) subtype are nonselective cation channels that are permeable to monovalent cations as well as to Ca^{2+}. Their Ca^{2+} permeability was first quantified by measurements of reversal potential shifts, which led to the estimation of relative permeabilities of Ca^{2+} over monovalent ions (P_{Ca}/P_M) (Mayer and Westbrook, 1987; Ascher and Nowak, 1988; Burnashev et al., 1992; Jahr and Stevens, 1993; Zarei and Dani, 1994), and later by simultaneous measurements of whole-cell current and Ca^{2+} influx, giving ratios of Ca^{2+} flux over total current (also called "fractional Ca^{2+} current" or P_f; Schneggenburger et al., 1993; Burnashev et al., 1995; Schneggenburger, 1996).

Despite the relatively detailed quantification of their Ca^{2+} permeability, the molecular mechanisms of Ca^{2+} and monovalent ion permeation through NMDA channels are not well understood. Soon after the cloning of NMDA channels (Moriyoshi et al., 1991; Monyer et al., 1992; Meguro et al., 1992), it was shown that mutagenesis of an asparagine residue located in the second hydrophobic domain (M2) of the NR1 subunit leads to a decrease in the relative Ca^{2+} permeability (Burnashev et al., 1992). In terms of the simplest hypothetical permeation model that assumes ion binding in the pore, a two-barrier, one-site model (see Fig. 1 *A*; Läuger, 1973; Lewis and Stevens, 1979; Hille, 1992), the effect of mutating an amino acid residue on relative Ca^{2+} permeability could be explained by a change in ionic selectivity at the outer, the inner, or both of the energy "barriers" that limit the flow of ions.

Received for publication 28 July 1997 and in final form 12 December 1997.

Address reprint requests to Dr. Ralf Schneggenburger, Abteilung Membranbiophysik, Max-Planck-Institut für Biophysikalische Chemie, Am Fassberg, 37077 Göttingen, Germany. Tel.: ++49-551-2011632; Fax: ++49-551-2011688; E-mail: rschneg@gwdg.de.

0006-3495/98/04/1790/05 $2.00

In wild-type NMDA channels composed of NR1 and NR2A subunits, the voltage dependence of fractional Ca^{2+} currents has been found to be in good agreement with the predictions of a two-barrier, one-site model (Schneggenburger, 1996), if it is assumed that the differences in barrier height for monovalent ions and Ca^{2+} are similar on the two sides of the membrane (constant peak energy offset condition; Lewis and Stevens, 1979; Hille, 1992). Interestingly, if a decrease in the relative Ca^{2+} permeability introduced by mutagenesis occurred exclusively because of an increase in the internal barrier height relative to that for monovalent ions, then the value of fractional Ca^{2+} current should increase with membrane hyperpolarization to the value observed in the wild-type channel (see Materials and Methods). To test this prediction, I analyzed a mutation (NR1E603K) at a site that can be expected to be located close to the internal membrane surface according to the three-transmembrane domain topology for glutamate receptor channels (Hollmann et al., 1994).

MATERIALS AND METHODS

Experimental procedures

Experiments were performed using the rat NMDA-receptor subunits NR1 and NR2A, which were kindly provided by the laboratories of S. Nakanishi (NR1; Moriyoshi et al., 1991) and P. Seeburg (NR2A; Monyer et al., 1992). The cDNAs were subcloned into a modified expression vector (pcDNA3; InVitrogen, Leek, the Netherlands), and point mutations were introduced as described by Kupper et al. (1996). NR1 and NR2A subunits were expressed in human embryonic kidney (HEK) cells according to the calcium phosphate precipitation method, using a cDNA ratio of 1:3 (NR1:NR2A). Green fluorescent protein (GFP) (Marshall et al., 1995) was cotransfected to facilitate the screening of cells expressing NMDA channels. Cells were used within 12–48 h after transfection.

Whole-cell patch-clamp recordings (Hamill et al., 1981) were made at room temperature (20–22°C), using an EPC-7 amplifier (List-electronics, Darmstadt, Germany) and data acquisition software (PClamp6; Axon Instruments, Foster City, CA). Internal solutions were composed of 140 mM CsCl, 10 mM HEPES, 5 mM Cs_2-EGTA for reversal potential measure-

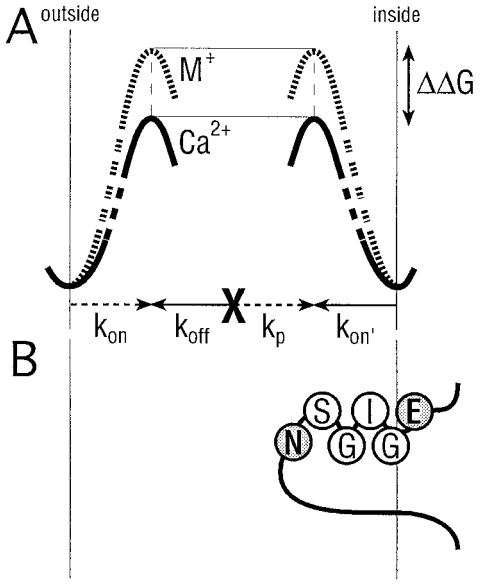

FIGURE 1 (*A*) A two-barrier one-site model for fractional Ca^{2+} currents. In this simplest case of a one-ion channel model, relative Ca^{2+} permeability (P_{Ca}/P_M) and fractional Ca^{2+} current (P_f) are determined by the difference in barrier height ($\Delta\Delta G$) for monovalent ions (M^+) and Ca^{2+}. The rate constants used in Eq. 2 (see Materials and Methods) are indicated by arrows. (*B*) Hypothetical arrangement of the M2 segment according to the three-domain model of glutamate receptor transmembrane topology (Hollmann et al., 1994). The amino acid residues of the NR1 subunit are shown in one-letter code in a region between asparagine 598 and glutamate 603. Note that the negatively charged glutamate (E) residue comes to lie close to the internal membrane side according to this model.

ments, or 145 mM CsCl, 10 mM HEPES, 1 mM K_5-fura-2 (Molecular Probes, Eugene, OR) (pH 7.2 in both cases) for measuring fractional Ca^{2+} currents. The extracellular solution contained 150 mM NaCl, 10 mM HEPES, 0.1–10 mM $CaCl_2$, and 0.1 mM glycine (pH 7.4).

A typical measurement of fractional Ca^{2+} currents consisted of the following procedures. First, a single, GFP-positive cell was placed into the circular area (diameter 50 μm) from which the photomultiplier tube collected its fluorescence light input. A pipette (resistance of 2–3 MΩ) was sealed onto the cell, and the fluorescence values at 360- and 380-nm excitation (after a short waiting period of ~30 s) were taken as background. The cell was then loaded with fura-2 in the whole-cell mode, until stable fluorescence values were reached (~5 min with access resistances ranging between 4 and 7 MΩ). In cells that had seal resistances of $\geq$1 GΩ, low basal $[Ca]_i$ values, and NMDA responses in the range of 0.2–2 nA, measurements of fractional Ca^{2+} currents were then made at various membrane potentials (beginning at -50 mV), until the reversal potential of the current response was reached. Successive applications of NMDA were carried out at intervals of ~1 min to allow for the (slow) relaxation of peak $[Ca]_i$ values back to baseline. At the end of the experiment, the cell was visually inspected through the eyepieces of the microscope. In a few cases, two closely contacting, presumably dividing cells were encountered. Such cells were rejected from the final data pool.

For analysis, membrane potential was given relative to the calculated reversal potential of the monovalent current component, taking into account the (small) liquid junction potential shift induced by adding extracellular $CaCl_2$ (Schneggenburger, 1996). The ratio of the fluorescence change at 380-nm excitation wavelength divided by the whole-cell charge ("FQ ratio," given in units of BU/nC) was calculated and transformed into a value of fractional Ca^{2+} current. The reference FQ ratio (8 BU/nC) was estimated previously from measurements in wild-type NMDA channels on the same experimental set-up (Schneggenburger, 1996).

Data are reported as average values $\pm$ standard deviation. The dependence of reversal potentials on extracellular Ca^{2+} concentration (Fig. 2) was fitted by the Goldman-Hodgkin-Katz (GHK) voltage equation extended for the use of divalent ions (Jan and Jan, 1976), without correcting for ionic activities.

Predictions from a two-barrier one-site model

To obtain a prediction for the effects of ion selectivity changes that occur preferentially on one membrane side, the simplest case of a one-ion channel model for the NMDA channel (Zarei and Dani, 1994) is considered. We want to find an expression for the ratio of the Ca^{2+} current component (I_{Ca}) over the monovalent current component (I_M) through a population of channels with one type of permeation pathway. The current ratio I_{Ca}/I_M can be transformed into P_f according to the definition $P_f = I_{Ca}/(I_{Ca} + I_M)$ (Schneggenburger et al., 1993).

Consider the case of a two-barrier, one-site model with monovalent ions inside and outside and Ca^{2+} ions outside (see Fig. 1 *A*). The probability of occupancy of the site with ion x (p_x) divided by the probability that the site is unoccupied (p_0) is given by

$$\frac{p_x}{p_0} = \frac{k_{on,x} \cdot C_{o,x} + k_{on',x} \cdot C_{i,x}}{k_{off,x} + k_{p,x}} \quad (1)$$

where $k_{on,x}$ and $k_{on',x}$ are on-rate constants, $k_{p,x}$ and $k_{off,x}$ are off-rate constants (see Fig. 1 *A*), and $C_{o,x}$ and $C_{i,x}$ denote external and internal concentration of ion x. Because in the stationary state the ion fluxes are equal for all barriers (Läuger, 1973), the current components I_M and I_{Ca} can be calculated by considering any one of the two barriers. For the outer barrier one obtains $I_x = zF\,(p_x \cdot k_{off,x} - p_0 \cdot k_{on,x} \cdot C_{o,x})$ (Lewis and Stevens, 1979). The current ratio can then be obtained by dividing the expression for I_{Ca} by the one for I_M. By dividing all terms by p_0 and replacing the resulting ratios p_{Ca}/p_0 and p_M/p_0 with the corresponding expressions of Eq. 1, and by further dividing all terms by $k_{on,M} \cdot [M]_o$, one obtains

$$\frac{I_{Ca}}{I_M} = \frac{\dfrac{2k_{on,Ca} \cdot [Ca]_o}{k_{on,M} \cdot [M]_o}\left(1 - \left(1 + \dfrac{k_{p,Ca}}{k_{off,Ca}}\right)^{-1}\right)}{1 - \left(1 + \dfrac{k_{on',M} \cdot [M]_i}{k_{on,M} \cdot [M]_o}\right)\left(1 + \dfrac{k_{p,M}}{k_{off,M}}\right)^{-1}} \quad (2)$$

From this equation it is seen that the current ratio does not depend on the absolute values of the rate constants or on the occupancy of the ion binding site. This is expected for any model which assumes that only one ion can occupy the channel at a given time.

The rate constants depend exponentially on membrane potential (Hille, 1992), and rate constants describing inward cation movement ($k_{on,x}$, $k_{p,x}$) have voltage dependencies opposite those describing outward cation movement ($k_{on',x}$, $k_{off,x}$). Considering the voltage-dependent changes in the different terms of Eq. 2, it can then be seen that in the limit of large negative potentials, the current ratio approaches

$$\frac{I_{Ca}}{I_M} = \frac{2k_{on,Ca} \cdot [Ca]_o}{k_{on,M} \cdot [M]_o} \quad (3)$$

Thus, in a mutant channel in which the relative Ca^{2+} permeability is decreased by a moderate reduction of the permeation rate for Ca^{2+} ($k_{p,Ca}$), but in which the ratio of the on-rate constants for Ca^{2+} and Na^+ is unchanged, P_f will recover with membrane hyperpolarization to the value observed in the wild-type channels, as was observed for the mutants studied here (see Fig. 3 *B*).

In Fig. 3 *B*, some model predictions for fractional Ca^{2+} currents are shown. The dashed lines represent the predictions for the constant peak energy offset case, with values for P_{Ca}/P_M of 3.6 (*upper dashed line* in Fig. 3 *B*) and 1.6 (*lower dashed line* in Fig. 3 *B*). The solid line was calculated assuming that the reduction in Ca^{2+} permeability occurred exclusively by elevating the internal barrier for Ca^{2+}. Note that in this case, P_f values recover to the value of the wild-type channel with membrane hyperpolar-

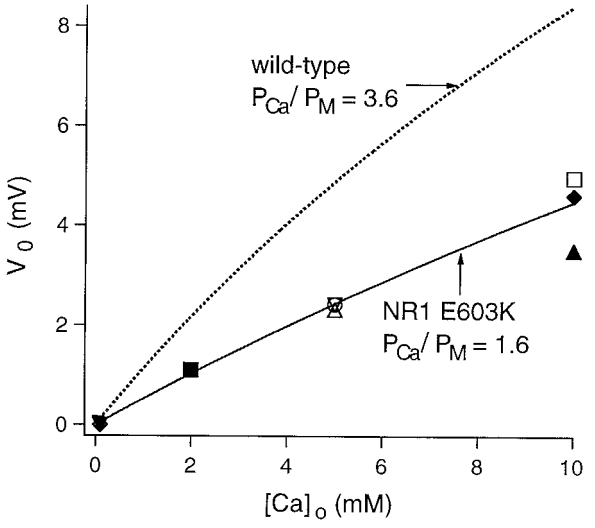

FIGURE 2 Ca^{2+}-induced reversal potential shifts in NR1E603K mutant channels. Reversal potentials were measured at three different $[Ca]_o$ (0.1 mM, 5 mM, and 10 mM) relative to the value at 2 mM $[Ca]_o$. The results from $n = 9$ cells are shown. The data were fitted with the Goldman-Hodgkin-Katz voltage equation, giving $P_{Ca}/P_M = 1.6$ (without correcting for ionic activities). The fit for the data obtained under the same experimental conditions for the wild-type channels (Schneggenburger, 1996) is shown for comparison.

ization. The model predictions were calculated according to Eq. 2 by using energy barrier heights at 0 mV from which the voltage-dependent rate constants were computed. The following simplifying assumptions were made: 1) P_{Cs} was assumed to be equal to P_{Na} ($P_{Cs} = P_{Na} = P_M$), and the energy barrier heights for monovalent ions were assumed to be equal at 0 mV. 2) The electrical distance of the ion binding site was arbitrarily set to 0.5. Although under these simplifying assumptions the asymmetrical one-site model (*solid line* in Fig. 3 *B*) did not yield a perfect fit of the data, no attempts were made to adjust the fit parameters of the one-site model, because the possibility cannot be excluded at present that a model with a larger number of free parameters (i.e., with more than one binding site) would give a significantly better fit of the data.

RESULTS AND DISCUSSION

Ca^{2+}-induced reversal potential shifts, measured in NR1E603K-NR2A mutant channels expressed in HEK cells, were smaller than those observed with wild-type channels. The dependence of reversal potentials on external Ca^{2+} concentration ($[Ca]_o$; range 0.1–10 mM, $n = 9$ cells) was well described by the extended GHK-voltage equation with a P_{Ca}/P_M value of 1.6 (Fig. 2), compared to a value of 3.6 obtained for the wild-type channel under similar conditions (Schneggenburger, 1996; see *dashed line* in Fig. 2). Thus the relative permeability of Ca^{2+} over monovalent ions, as measured by reversal potential shifts close to 0 mV, was reduced by a factor of ~2 with respect to the wild-type channel.

As a second measure of relative Ca^{2+} permeability, the ratio of Ca^{2+} current over total ionic current (fractional Ca^{2+} current) was measured at membrane potentials of −50 mV and at 2 mM $[Ca]_o$. For these experiments, HEK cells expressing the mutant NR1E603K channels were loaded

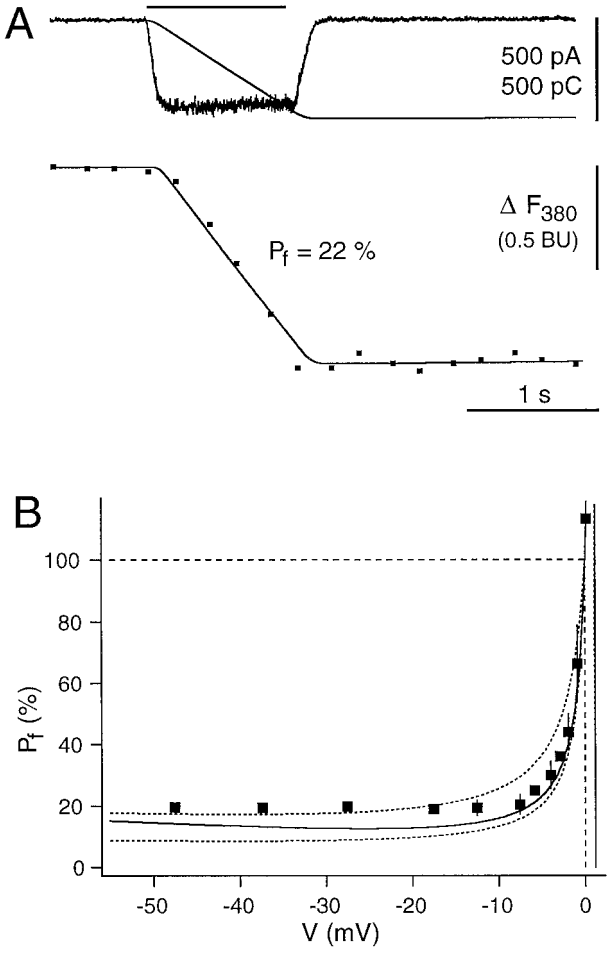

FIGURE 3 Voltage dependence of fractional Ca^{2+} currents through the NR1E603K mutant channels. (*A*) Example of a measurement at −50 mV. NMDA (50 μM) was applied during the time indicated by the horizontal bar. The smooth line in the upper panel indicates the time integral of the NMDA-induced current. The factor from scaling the time integral to the measured fluorescence at 380-nm excitation wavelength (F_{380}, *dots in lower panel*) gives the FQ ratio, from which a fractional Ca^{2+} current of 22% was calculated. (*B*) Fractional Ca^{2+} current (P_f) as a function of membrane potential. Each data point represents the average value from measurements in three cells. Membrane potential is given relative to the calculated reversal potential of the monovalent current component, and values between different cells were grouped and averaged. The predictions from a two-barrier, one-site model under the constraint of constant peak energy offset are shown for two relative Ca^{2+} permeabilities (P_{Ca}/P_M = 3.6 and 1.6; *upper and lower dashed lines*, respectively). The solid line gives the prediction from a model in which the constant peak energy offset condition was relaxed (see Materials and Methods, $P_{Ca}/P_M = 1.6$).

nearly completely (≥5 min of whole-cell recording) with 1 mM fura-2, a high-affinity ($K_d \approx 200$ nM) Ca^{2+} indicator dye. Under these conditions and at internal free Ca^{2+} concentrations less than 200 nM, changes in the Ca^{2+}-dependent fluorescence at 380-nm excitation were used to measure the time integral of Ca^{2+} influx after the activation of whole-cell NMDA currents. As can be seen in Fig. 3 *A*, a strong Ca^{2+} influx signal was observed after the activation of NR1E603K mutant channels. The FQ ratio of this response, which was derived by scaling the time integral of

the current response to the fluorescence signal, was divided by the reference FQ ratio to yield an estimation of the fractional Ca^{2+} current. In the example of Fig. 3 *A*, fractional Ca^{2+} current was 22%, and on average a value of 19.7 ± 1% was found ($n = 3$ cells).

This value is comparable to the value reported earlier under similar experimental conditions for the wild-type channel (18.5 ± 1.3%; Schneggenburger, 1996; see Table 1), although the relative permeability P_{Ca}/P_M of the mutant channel, as estimated from reversal potential measurements close to 0 mV, is reduced by a factor of ~2 with respect to the wild-type channel (Fig. 2). To characterize the voltage dependence of fractional Ca^{2+} currents through the NR1E603K mutant channels, measurements were made between −50 mV and the reversal potential of the NMDA whole-cell responses. The average results of three experiments are shown in Fig. 3 *B*. Whereas the values close to the reversal potential are well described by the constant peak energy offset prediction for a value of P_{Ca}/P_M of 1.6 (*lower dashed line* in Fig. 3 *B*), at membrane potentials more negative than −10 mV, fractional Ca^{2+} currents significantly deviated from this prediction, approaching the values observed earlier for the wild-type channels. For comparison, the constant peak energy offset prediction used previously for the wild-type channels with a P_{Ca}/P_M value of 3.6 (Schneggenburger, 1996) is also displayed (*upper dashed line* in Fig. 3 *B*).

Thus, whereas the voltage dependence of fractional Ca^{2+} currents through wild-type NMDA channels can be adequately described assuming constant peak energy offset conditions (Schneggenburger, 1996), this assumption clearly fails to explain the voltage dependence of fractional Ca^{2+} currents through the NR1E603K mutant channels. This finding can be interpreted in terms of a two-barrier, one-site model if it is assumed that the permeation rate ($k_{p,Ca}$), but not the on-rate for Ca^{2+} ions ($k_{on,Ca}$), was affected by the mutagenesis (see Materials and Methods). Then P_f values are expected to recover with membrane hyperpolarization to the values observed in wild-type channels (see Materials and Methods). The result of this analysis is compatible with the three-transmembrane domain topology of glutamate receptor channels (Hollmann et al., 1994; see also Kupper et al., 1996; Kuner et al., 1996), which places the NR1E603 residue close to the internal membrane side.

On the other hand, the finding that the charge inversion mutation at the NR1E603 site had a relatively weak overall effect on Ca^{2+} permeability is incompatible with a strong role of this amino acid residue in Ca^{2+} permeation. Indeed, Burnashev et al. (1992) showed that by introducing a positively charged arginine at the asparagine site of the NR1 subunit (NR1N598R mutation), the Ca^{2+} permeability of the resulting mutant channels was completely abolished. This indicates that the asparagine residue of the NR1 subunit is probably more directly involved in the ion permeation process (see also Wollmuth et al., 1996; Kuner et al., 1996). Therefore, I was interested in screening mutations at the asparagine sites of the NR1 and the NR2A subunits for moderate reductions of relative Ca^{2+} permeability, which would allow the measurement of fractional Ca^{2+} currents over an extended membrane potential range.

The results of these measurements are listed in Table 1. A serine substitution in the NR1 subunit (NR1N598S) showed only small fractional Ca^{2+} currents at negative membrane potentials and was not studied further. However, two cysteine substitutions of asparagine residues in the NR1 and NR2A subunits showed moderate reductions in P_{Ca}/P_M, and the values for fractional Ca^{2+} currents at negative membrane potentials were found to be larger than the ones predicted under the assumption of constant peak energy offset, as in the NR1E603K mutant.

The quantitative modeling of fractional Ca^{2+} currents for the point mutations at the asparagines in the M2 domain is, unfortunately, complicated by the finding that mutations at these positions can introduce subconductance states with high open probability and ion selectivity properties different from those of the main states (Premkumar and Auerbach, 1996; Schneggenburger and Ascher, 1997). Whole-cell ion permeability measurements, like measurements of reversal potentials and fractional Ca^{2+} currents, would then represent average measurements from two conductance states with different selectivity properties. The NR1E603K mutant did not show such anomalous subconductance states (see Kupper et al., 1996). Nevertheless, it is seen that similar effects on Ca^{2+} selectivity were observed for the mutations at the asparagine 598 site and for the much more drastic, charge inversion mutation at the glutamate 603 site (see Table 1). It therefore seems plausible to assume that the charge inversion at glutamate 603 has an electrostatic effect on an internal barrier to ion permeation that might be formed by the asparagines (Wollmuth et al., 1996; Kuner et al., 1996) in the M2 domains of the NR1 and NR2A subunits.

TABLE 1 Fractional Ca^{2+} currents and relative Ca^{2+} permeabilities in some NMDA channel pore mutants

Channel type	P_f (%)	P_{Ca}/P_M	Relative P_f*
Wild type	18.5 ± 1.3 (8)[#]	3.6	1.06 ± 0.07
NR1E603K	19.7 ± 1 (3)	1.6	2.29 ± 0.12
NR1N598C	20.2 ± 0.9 (3)	1.7[§]	2.13 ± 0.1
NR2AN595C	11.9 ± 0.6 (3)	1.0[§]	2.16 ± 0.12
NR1N598S	2.7 ± 0.3 (3)	ND	ND

Fractional Ca^{2+} currents (P_f) at −50 mV and 2 mM $[Ca]_o$. Values in brackets refer to the number of cells studied. ND: not determined.

*Fractional Ca^{2+} currents relative to the prediction of a two-barrier, one-site model under constant peak energy offset conditions for the corresponding P_{Ca}/P_M value.

[#]Data from Schneggenburger (1996).

[§]Values estimated from P_f measurements close to 0 mV.

I thank Drs. J. Kupper, J. Neyton, and P. Ascher for discussing the data and for helpful comments on the manuscript, and Dr. J. Neyton for generous help with mutagenesis and for providing some of the mutant clones studied here.

This work was supported by the Centre National de la Recherche Scientifique (URA 1857) and by postdoctoral fellowships from the European Union (HCM program) and the Fondation de la Recherche Medicale.

REFERENCES

Ascher, P., and L. Nowak. 1988. The role of divalent cations in the *N*-methyl-D-aspartate responses of mouse central neurones in culture. *J. Physiol. (Lond.).* 399:247–266.

Burnashev, N., R. Schoepfer, H. Monyer, J. P. Ruppersberg, W. Günther, P. H. Seeburg, and B. Sakmann. 1992. Control by asparagine residues of calcium permeability and magnesium blockade in the NMDA receptor. *Science.* 257:1415–1419.

Burnashev, N., Z. Zhou, E. Neher, and B. Sakmann. 1995. Fractional calcium currents through recombinant GluR channels of the NMDA, AMPA and kainate receptor subtypes. *J. Physiol. (Lond.).* 485:403–418.

Hamill, O. P., A. Marty, E. Neher, B. Sakmann, and F. J. Sigworth. 1981. Improved patch-clamp techniques for high-resolution current recording from cells and cell-free membrane patches. *Pflügers Arch.* 393: 254–261.

Hille, B. 1992. Ionic Channels of Excitable Membranes. Sinauer Associates, Sunderland, MA.

Hollmann, M., C. Maron, and S. Heinemann. 1994. *N*-Glycosylation site tagging suggests a three transmembrane domain topology for the glutamate receptor GluR1. *Neuron.* 13:1331–1343.

Jahr, C. E., and C. F. Stevens. 1993. Calcium permeability of the *N*-methyl-D-aspartate receptor channel in hippocampal neurons in culture. *Proc. Natl. Acad. Sci. USA.* 90:11573–11577.

Jan, L. Y., and Y. N. Jan. 1976. L-Glutamate as an excitatory transmitter at the *Drosophila* neuromuscular junction. *J. Physiol. (Lond.).* 262: 215–236.

Kuner, T., L. Wollmuth, A. Karlin, P. H. Seeburg, and B. Sakmann. 1996. Structure of the NMDA receptor channel M2 segment inferred from the accessibility of substitued cysteines. *Neuron.* 17:343–352.

Kupper, J., P. Ascher, and J. Neyton. 1996. Probing the pore region of recombinant *N*-methyl-D-aspartate channels using external and internal magnesium block. *Proc. Natl. Acad. Sci. USA.* 93:8648–8653.

Läuger, P. 1973. Ion transport through pores: a rate-theory analysis. *Biochim. Biophys. Acta.* 311:423–441.

Lewis, C. A., and C. F. Stevens. 1979. Mechanism of ion permeation through channels in a postsynaptic membrane. *In* Membrane Transport Processes. C. F. Stevens and R. W. Tsien, editors. Raven Press, New York. 133–151.

Marshall, J., R. Molloy, G. W. Moss, J. R. Howe, and T. E. Hughes. 1995. The jellyfish green fluorescent protein: a new tool for studying ion channel expression and function. *Neuron.* 14:211–215.

Mayer, M. L., and G. L. Westbrook. 1987. Permeation and block of *N*-methyl-D-aspartatic acid receptor channels by divalent cations in mouse cultured central neurones. *J. Physiol. (Lond.).* 394:501–527.

Meguro, H., H. Mori, K. Araki, E. Kushiya, T. Kutsuwada, M. Yamazaki, T. Kumanishi, M. Arawaka, K. Sakimura, and M. Mishina. 1992. Functional characterization of a heteromeric NMDA receptor channel expressed from cloned cDNAs. *Nature.* 357:70–74.

Monyer, H., R. Sprengel, R. Schoepfer, A. Herb, M. Higuchi, H. Lomeli, N. Burnashev, B. Sakmann, and P. H. Seeburg. 1992. Heteromeric NMDA receptors: molecular and functional distinction of subtypes. *Science.* 256:1217–1221.

Moriyoshi, K., M. Masu, T. Ishii, R. Shigemoto, N. Mizuno, and S. Nakanishi. 1991. Molecular cloning and characterization of the rat NMDA receptor. *Nature.* 354:31–37.

Premkumar, L. S., and A. Auerbach. 1996. Identification of a high affinity divalent cation binding site near the entrance of the NMDA receptor channel. *Neuron.* 16:869–80.

Schneggenburger, R. 1996. Simultaneous measurement of Ca^{2+} influx and reversal potentials in recombinant *N*-methyl-D-aspartate receptor channels. *Biophys. J.* 70:2165–2174.

Schneggenburger, R., and P. Ascher. 1997. Coupling of permeation and gating in an NMDA-channel pore mutant. *Neuron.* 18:167–177.

Schneggenburger, R., Z. Zhou, A. Konnerth, and E. Neher. 1993. Fractional contribution of calcium to the cation current through glutamate receptor channels. *Neuron.* 11:133–143.

Wollmuth, L. P., T. Kuner, P. H. Seeburg, and B. Sakmann. 1996. Differential contribution of the NR1- and NR2A-subunits to the selectivity filter of recombinant NMDA receptor channels. *J. Physiol. (Lond.).* 491:779–797.

Zarei, M. M., and J. A. Dani. 1994. Ionic permeability characteristics of the *N*-methyl-D-aspartate receptor channel. *J. Gen. Physiol.* 103:231–248.